GPS Solutions

Electronic supplementary material for

Satellite Laser Ranging to GNSS-based Swarm orbits with handling of systematic errors

Dariusz Strugarek[1] (0000-0001-7882-8105), Krzysztof Sośnica[1] (0000-0001-6181-1307), Daniel Arnold[2] (0000-0003-3574-0837), Adrian Jäggi[2], Radosław Zajdel[1] (0000-0002-1634-388X), Grzegorz Bury[1] (0000-0002-5816-410X)

[1] Wrocław University of Environmental and Life Sciences (UPWr), Institute of Geodesy and Geoinformatics, 25 Norwida St., 50-375 Wrocław, Poland

[2] Astronomical Institute, University of Bern, Sidlerstrasse 5, 3012 Bern, Switzerland

Corresponding author:

Dariusz Strugarek

e-mail: dariusz.strugarek@upwr.edu.pl; phone: +48 71 3205683

File description:

The supplementary material consists of the complementary analyses of estimated range and tropospheric biases, station coordinate corrections, and horizontal gradients, as well as SLR verification results for Swarm-A, and C satellites. All the nomenclatures and references are consistent with the main manuscript file. Figures S1, and S3-10 illustrate the Swarm-AC results in correspondence to Swarm-B results shown in the manuscript. Figure S2 considers supplementary results of parameter estimates for tested RB-D, TB+G, and RB+TB+G solutions of Swarm-ABC. Figures S11 and S12 show medians of estimated parameters and residual histograms for tested solutions to different orbit POD products of Swarm-B satellite, respectively.

Figure S1 depicts systematic effects in SLR residuals to Swarm-A, and -C, which correspond to Swarm-B results. For the Wettzell (7827) station and time-dependent analysis, the SLR residuals show a 10 mm offset for Swarm-A satellite. In the case of the Swarm-C satellite, the offset of residuals is 5 mm with occurrence of a few-mm increase over time. In the case of Graz (7839) station, the elevation angle dependency of residuals reaches -0.06 and -0.14 mm/°, for Swarm-A, and -C, respectively, with additional offset of residuals for Swarm-A satellite. The SLR residuals with respect to station-satellite azimuth-zenith angles for the Kunming station show high, +/- 40 mm variability of both Swarm-AC satellites.

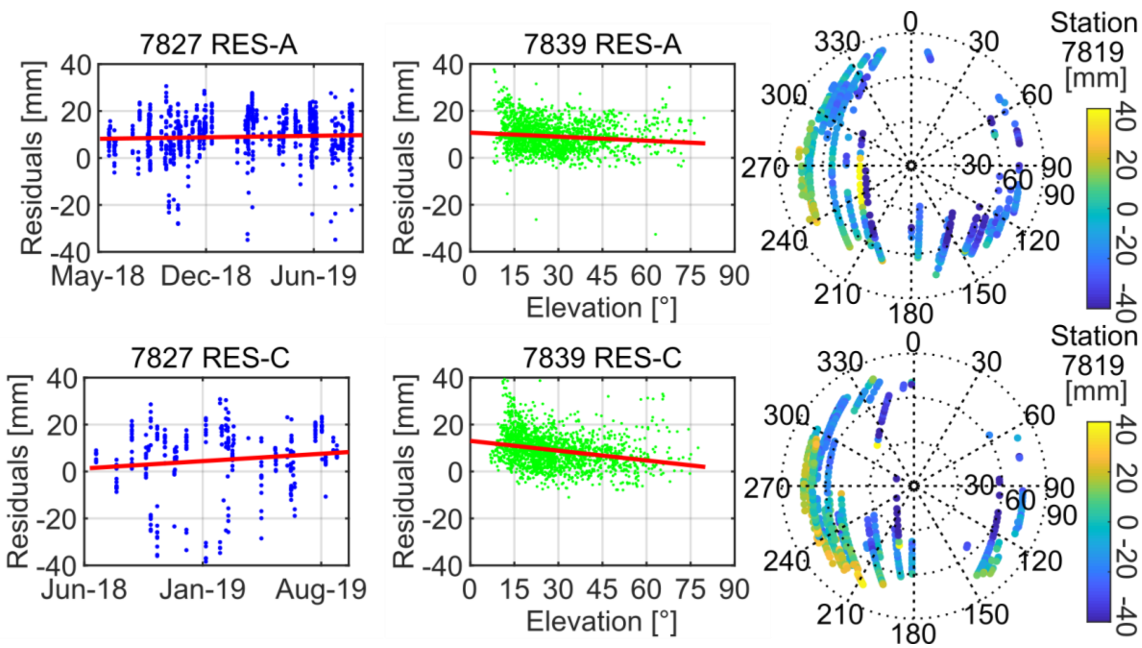

Fig. S1 Systematic effects in SLR residuals to Swarm-A (top) and Swarm-C (bottom) from Wettzell (7827), Graz (7839), and Kunming (7819) from June 2018 to August 2019 as a function of date, elevation angle, and station-satellite azimuth-zenith angles (0 degrees indicates the North direction) with fitted trend lines (in red)

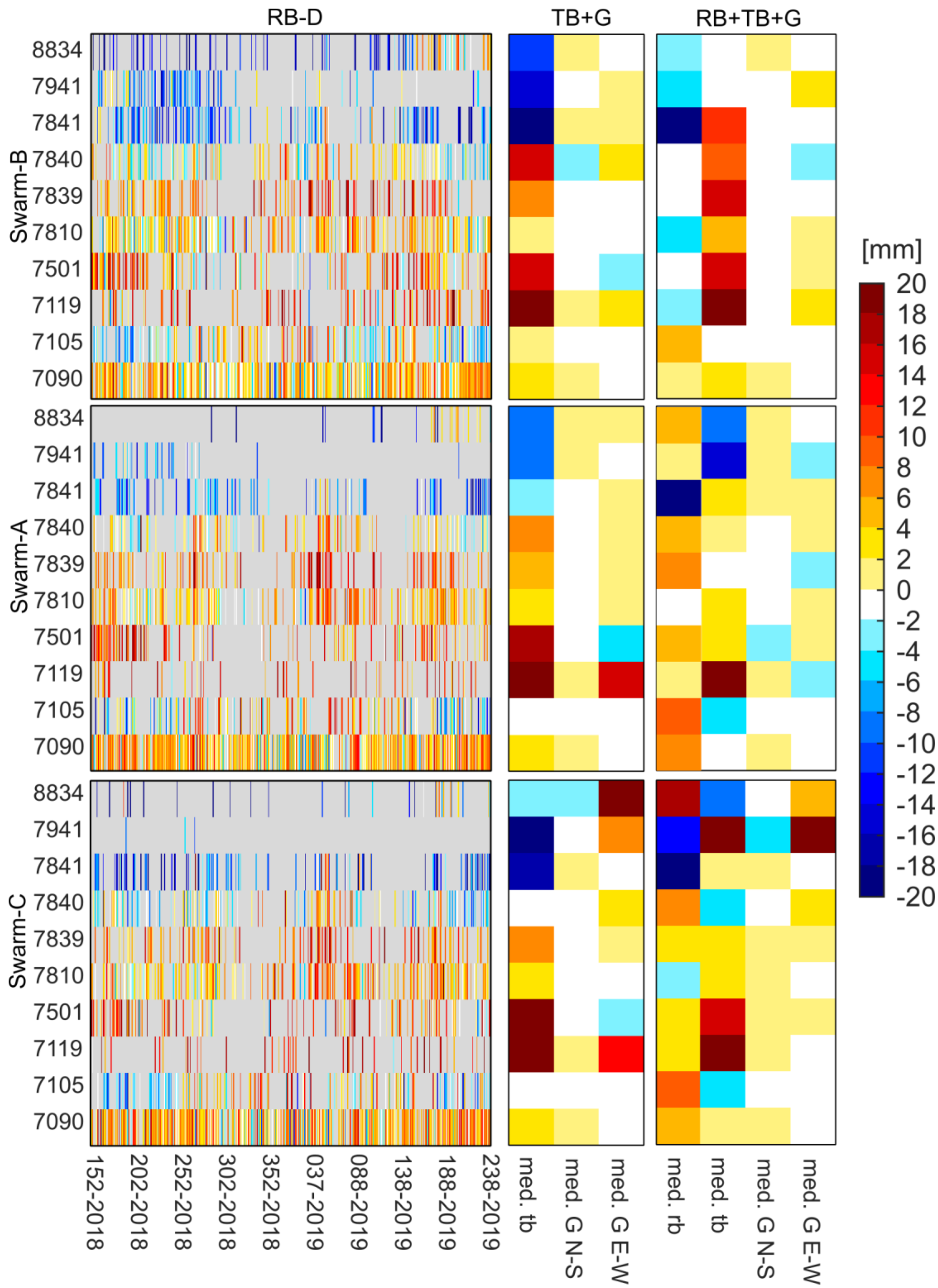

Fig. S2 Daily range biases and medians of estimated range, troposphere biases, and horizontal gradients for high-performing SLR stations, Swarm-ABC satellites and solutions RB-D, TB+G, and RB+TB+G. A gray area means no data

Figure S2 shows daily estimates of range bias parameters and median values of troposphere corrections, range biases and horizontal gradients for Swarm-ABC satellites and high-performing stations. The daily range biases from the RB-D solutions are stable in time for most of the stations, and consistent within Swarm constellation, e.g., 4-6 mm for 7090, -10 mm for 7841, despite the differences in the number of observations. However, in the case of 7840, 7810, 7105 stations, there are periods with only negative or only positive range biases, e.g., the 7105 station in days 152-252 of 2018 and between 252 of 2018 and 37 of 2019. The stations with range biases stable over time are more likely affected by errors of the SLR measurement system, or station coordinate determination errors, whereas time-dependent daily range biases suggest that measurements may be affected by other errors related to, e.g., troposphere modeling or geodynamical displacements.

The median tropospheric corrections for TB+G solutions are at the higher than TB solution in the range of +/-20 mm depending on stations, but show an increase of parameter differences to even 4-6 mm within the Swarm constellation. For 8834 and 7841, tropospheric bias inconsistencies relate to the large differences in the number of observations between Swarm-B and Swarm-AC. The median values of horizontal gradients from TB+G are within the range of +/- 4 mm with minor exceptions, however the Swarm-C results are less consistent with respect to the Swarm-A and -B satellites. In the case of the RB+TB+G solution, the median values of estimated troposphere corrections, and range biases show large variability, which are inconsistent within the Swarm constellation or other tested solutions. Only the horizontal gradients are within the range of +/- 4 mm. Moreover, the formal errors of estimated parameters from TB+G and RB+TB+G solution are within the range of a few mm to cm. Thus, estimating more than one daily parameter increases their noise and does not allow to identify what part of error is absorbed.

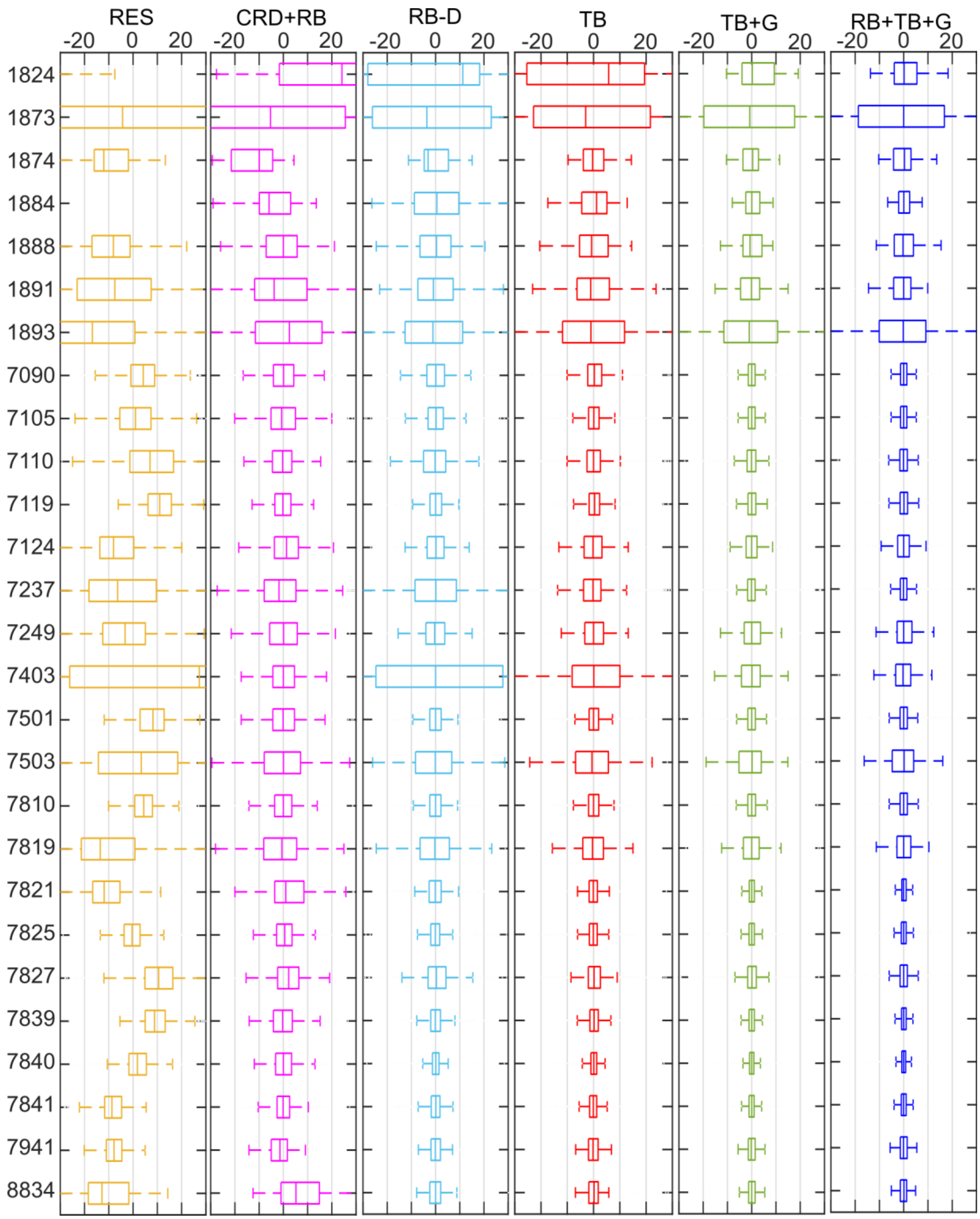

Fig. S3 Solution- and station-specific boxplots of SLR residuals to Swarm-A (median, 1st, 3rd quartile, max., and min. values, in mm)

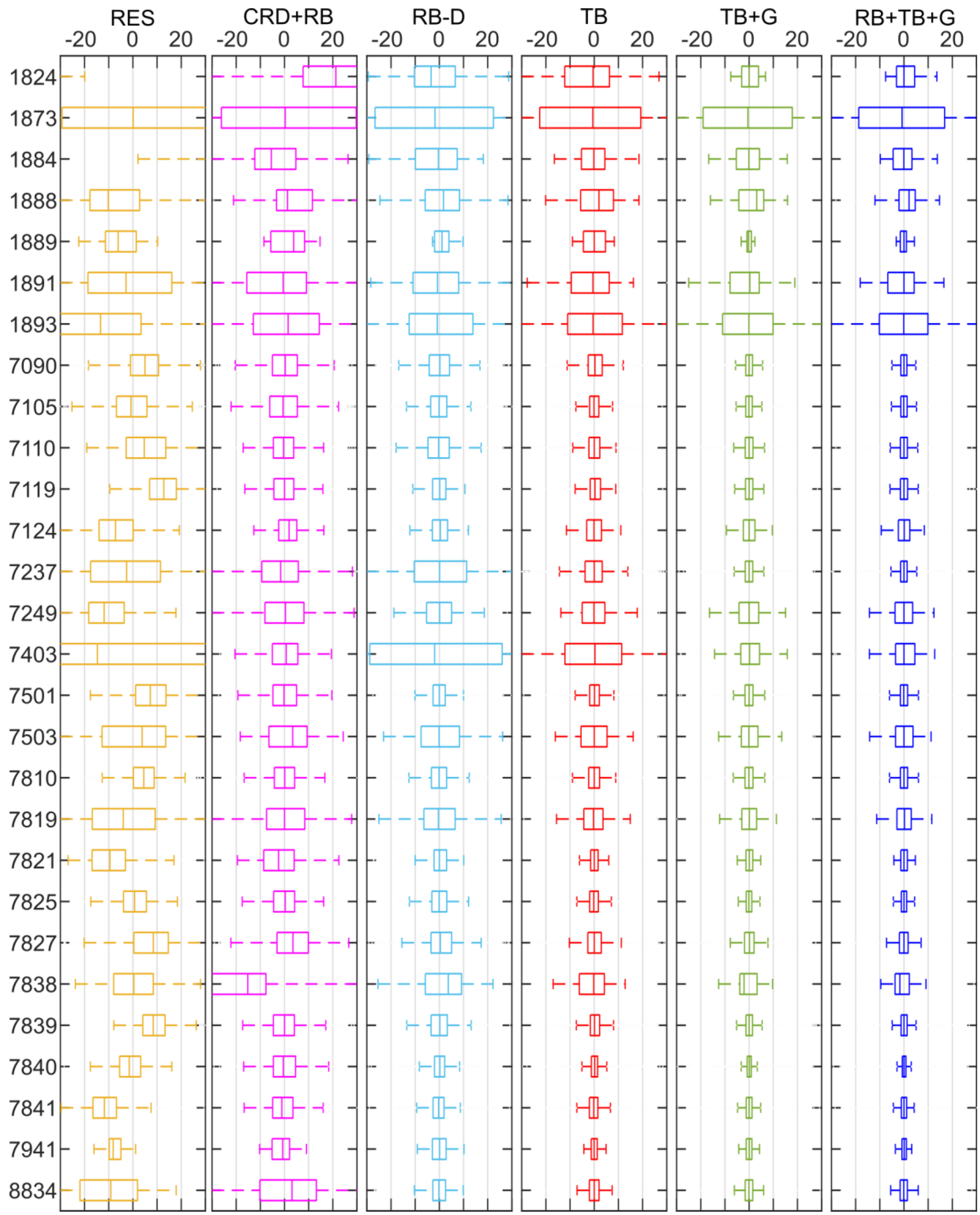

Fig. S4 Solution- and station-specific boxplots of SLR residuals to Swarm-C (median, 1st, 3rd quartile, max., and min. values, in mm)

Figures S3, S4 show boxplots of SLR residuals for all tested solutions, all stations and Swarm-AC satellites. In the case of Swarm-AC and RES solution, almost all stations are characterized with positive or negative offsets of residual medians and worse than 10 mm IQRs. As for the case of Swarm-B results (manuscript, Fig 4), modeling of systematic effects reduces offset of medians to near-zero values; however, in the case of CRD+RB and RB-D for some stations (e.g., 1889, 7503, 7838) the offsets of medians are still visible at a few mm level. The IQRs and medians for the TB solution are reduced for all stations and for Swarm-AC solution results. The additional estimation of horizontal gradients (TB+G), daily range biases with distance-dependent corrections (RB+TB+G) for Swarm-AC reduces the SLR residuals with respect to the TB solution, however, the level of reduction is less pronounced.

Figures S5, S6 show the SLR residuals as a function of time for Swarm-A and -C satellites and the Wettzell (7827) station in correspondence to Fig. 5 of the manuscript. In analogy to Swarm-B, the offset and dependency of residuals in RES solution are also successfully reduced to near-zero for all tested solutions and Swarm-AC satellites, with the largest reduction in residuals distribution for the TB, TB+G, and RB+TB+G solutions.

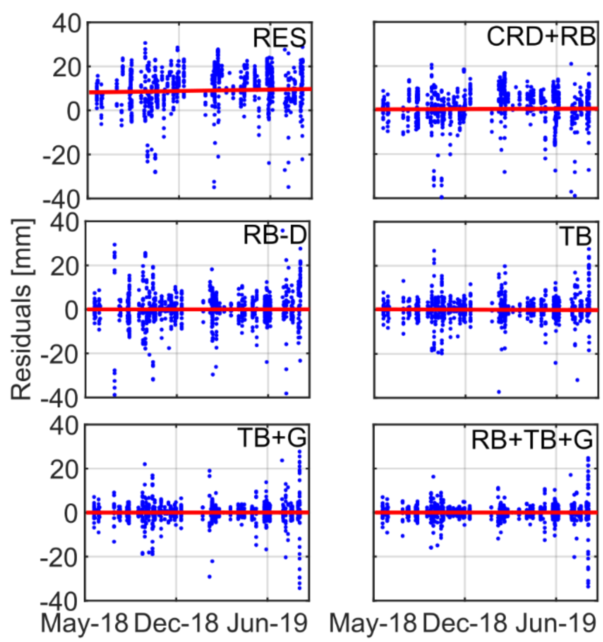

Fig. S5 SLR residuals with respect to time for Swarm-A and Wettzell (7827) station with fitted trend line (red)

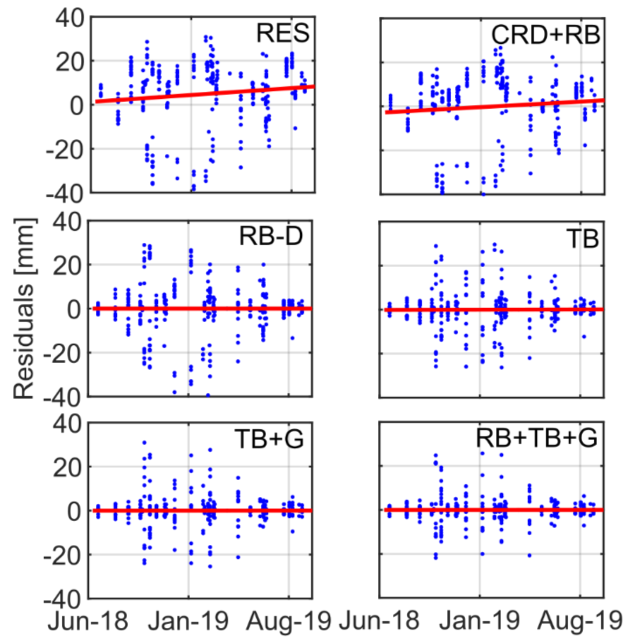

Fig. S6 SLR residuals with respect to time for Swarm-C and Wettzell (7827) station with fitted trend line (red)

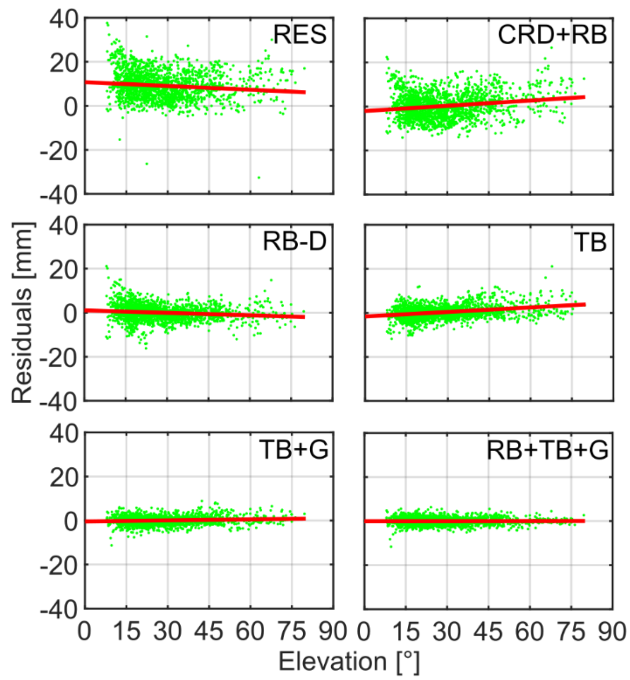

Fig. S7 SLR residuals with respect to station elevation angle for Swarm-A and the Graz (7839) station with fitted trend line (red).

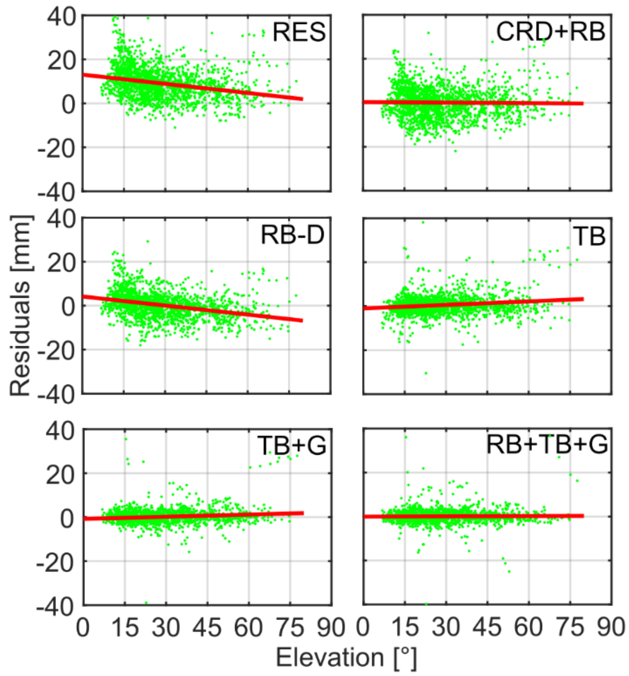

Fig. S8 SLR residuals with respect to station elevation angle for Swarm-C and the Graz (7839) station with fitted trend line (red).

Figures S7, S8 show the residuals with respect to elevation angle for Swarm-A and -C satellites, and the Graz (7827) station in correspondence to Fig. 6 of the manuscript. For Swarm-A, the offsets of residuals are reduced for all solutions, however, for CRD+RB, RB-D, and TB a few mm dependencies are still visible. For Swarm-C satellite, the elevation angle dependency is reduced in CRD+RB, TB, TB+G, and RB+TB+G solutions, whereas RB-D solution still shows a residual dependency of -0.13 mm/°. Nevertheless, the TB, TB+G, and RB+TB+G solutions successfully reduce the residual dependency with respect to RB-D and CRD+RB and diminish the spread of residuals to the lowest extent, similarly to the Swarm-B results.

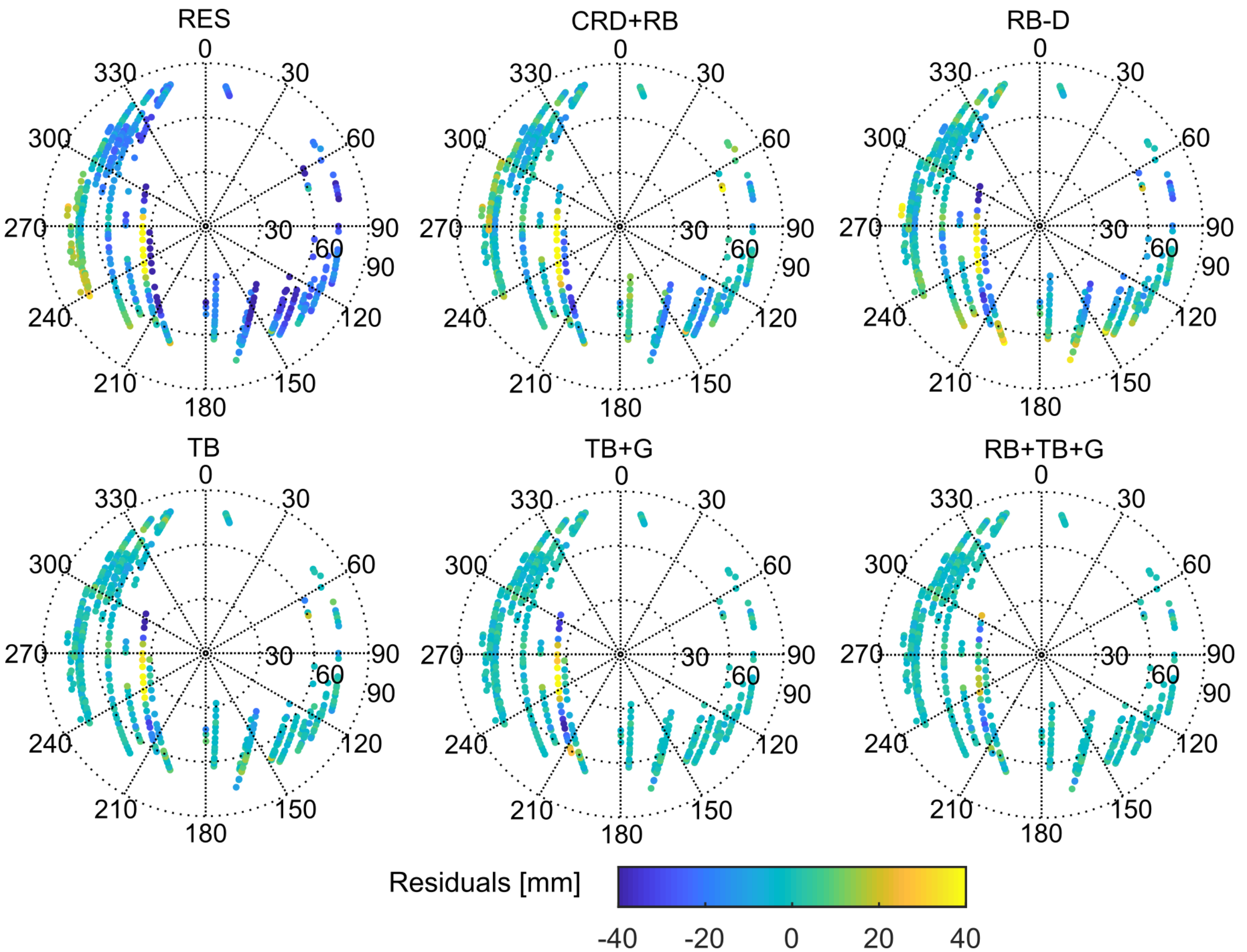

Fig. S9 SLR residuals with respect to station-satellite azimuth-zenith angles for Swarm-A and the Kunming (7819) station (0 degrees indicates the North direction)

Figures S9 and S10 show the SLR residuals with respect to station-satellite azimuth-zenith angles for Swarm-A, and -C satellites and the Kunming (7819) station in correspondence to Fig. 7 from the manuscript. In analogy to Swarm-B, the RES solutions show residual variability of -/+40 mm depending on station-satellite azimuth-zenith angles. For Swarm-AC, the CRD+RB and RB-D solutions successfully reduce some of the residual dependencies, but still, some passes and observations have large residual patterns. The TB, TB+G, and RB+TB+G solutions successfully reduce the residuals to the near-zero values, except for two anomalous passes in the case of Swarm-A and -B. However, these passes do not fall on the same days, i.e., 25-03-2019 for Swarm-A and 06-06-2019 for Swarm-B. Also, similar large residuals are not visible for corresponding passes for other stations closely located to Kunming, i.e., Changchun and Yarragadee. Moreover, for Swarm-C, the anomalous passes are not visible, which suggests that they are affected by gross SLR measurement errors, rather than satellite orbit errors.

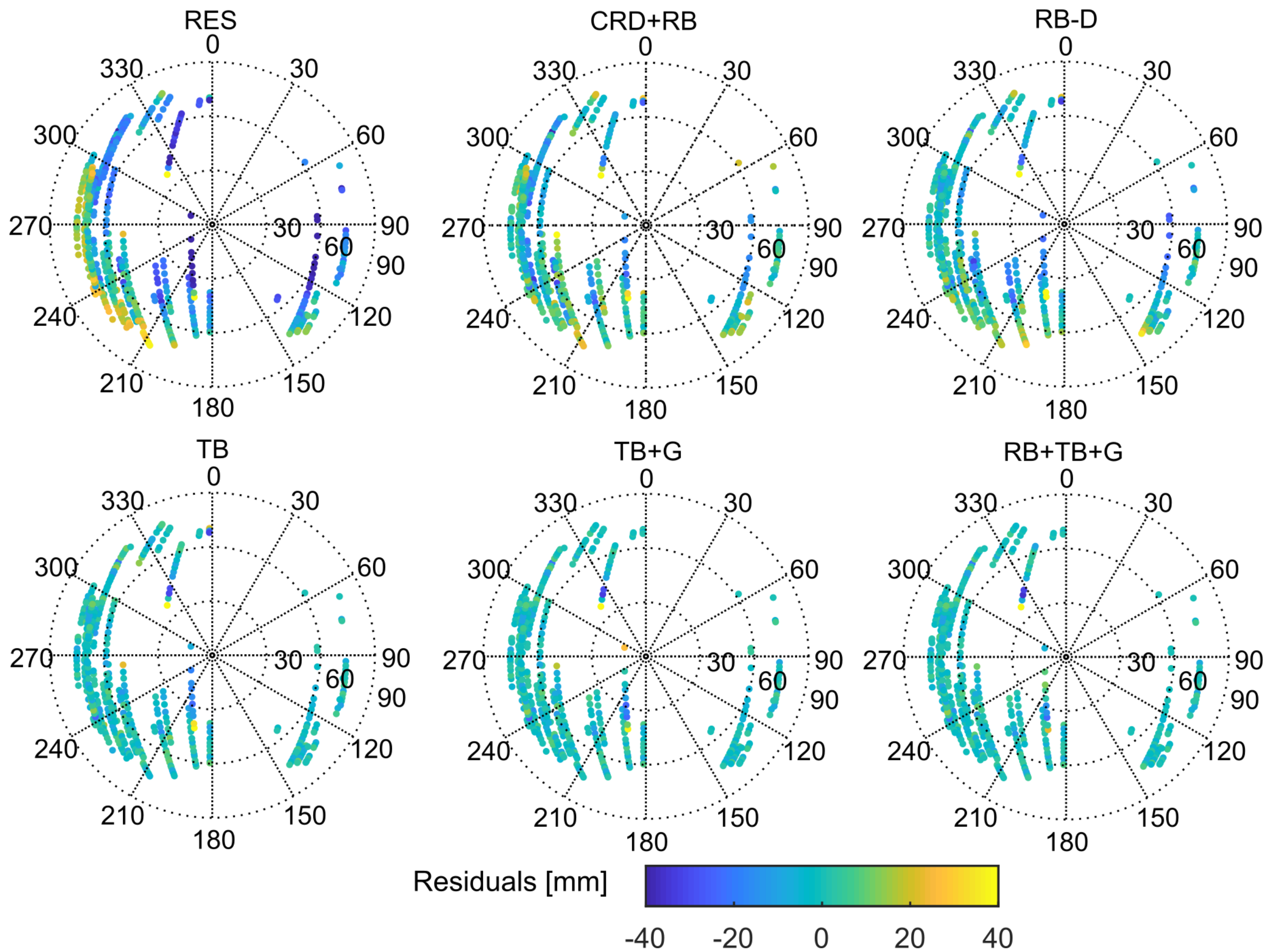

Fig. S10 SLR residuals with respect to station-satellite azimuth-zenith angles for Swarm-C and the Kunming (7819) station (0 degrees indicates the North direction)

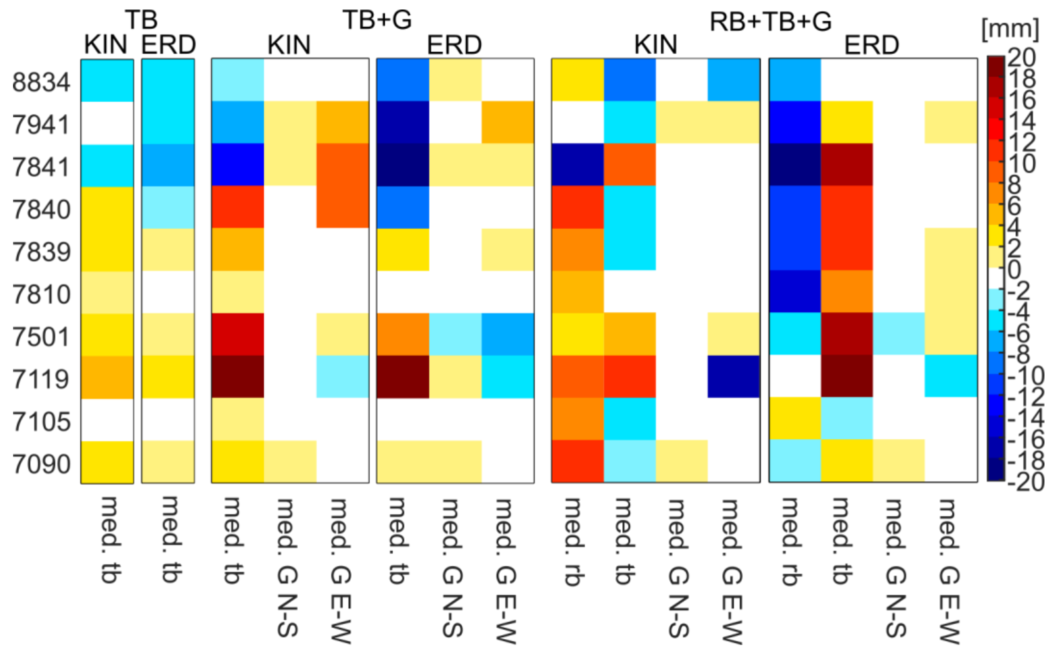

Fig. S11 Medians of estimated range, troposphere biases, and horizontal gradients for high-performing SLR stations, Swarm-B KIN and ERD orbits, and TB, TB+G, and RB+TB+G solutions

Fig. S11 shows the median values for estimated troposphere corrections, range biases, and horizontal gradients for solutions KIN and ERD, and Swarm-B satellite. Tropospheric corrections from TB solution are characterized with medians of +/- 6 mm for both KIN and ERD solutions, as well as estimates from TB solution in Fig. 4 (manuscript file), with minor differences of less than 1-2 mm. TB+G and RB+TB+G solutions show increased variability of +/-20 and +/-6 mm for the estimated troposphere/range bias corrections, and horizontal gradients, respectively, which do not correspond within analogical results of AIUB RD solutions within Swarm constellation (Fig. S2).

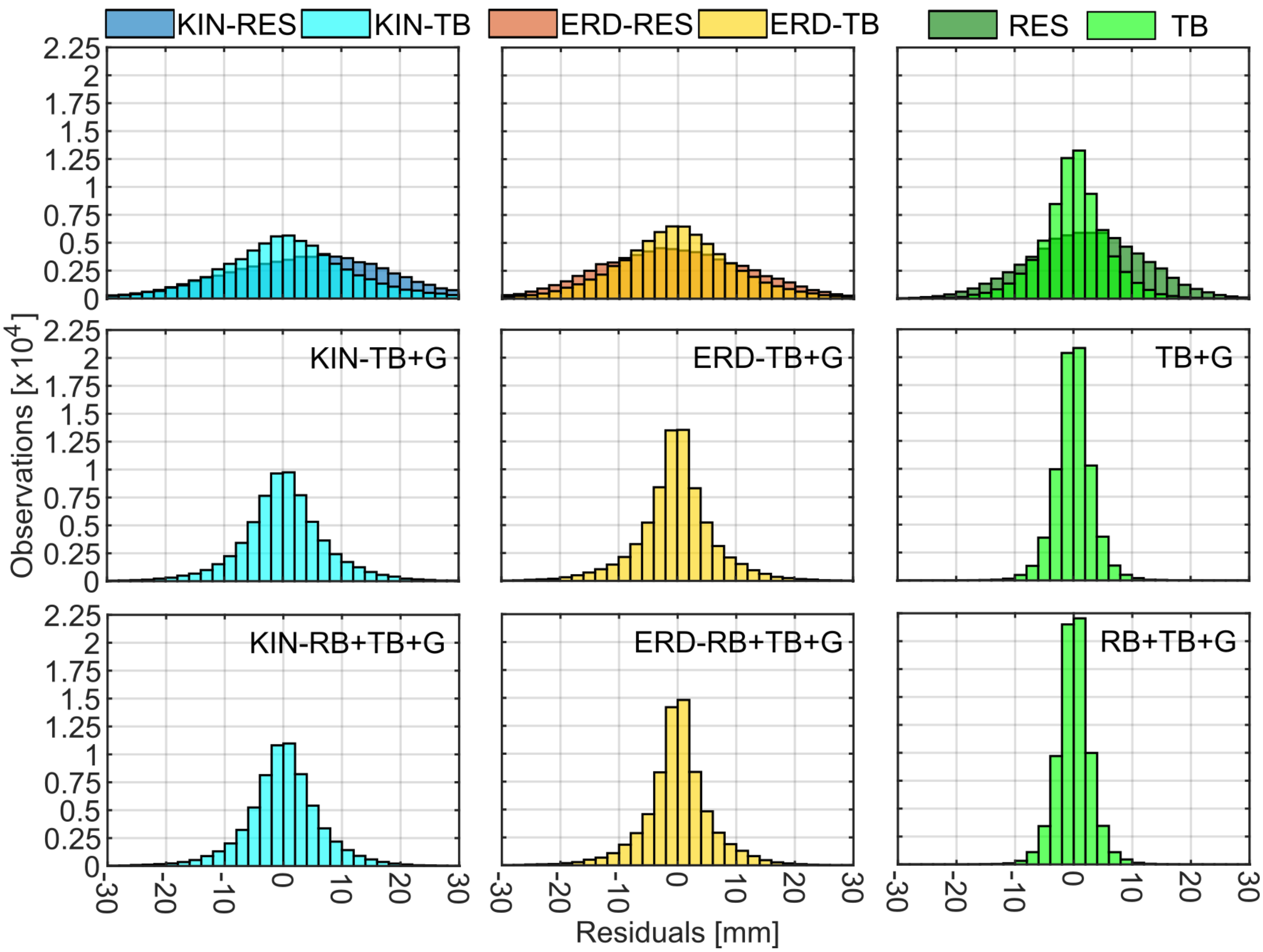

Fig. S12 Histogram of SLR observation residuals to Swarm-B based on KIN (blue, left), ERD (yellow, middle), AIUB RD (green, right) orbits, and TB, TB+G, and RB+TB+G solutions for high-performing SLR stations

Fig. S12 shows the histograms of SLR residuals for the reference RES solution (top row) for KIN, ERD, and AIUB RD POD products, and tested TB, TB+G, and RB+TB+G solutions. Estimates of troposphere correction (TB) reduce the offset and range of SLR residuals for all POD products; however, the most pronounced reduction effect is obtained for AIUB RD with 43,738 observations within the range of +/- 4 mm, which is almost two times more than in RES solution. POD-dependent reduction of residual distribution in histograms also occurs for solutions considering more than one additional parameter in TB, i.e., horizontal gradients (TB+G) and range biases (RB+TB+G). However, estimating additional range biases (RB+TB+G) gives just minor improvement when compared to the TB+G. The distribution of all residuals in histograms is reduced to the range of +/- 10 mm for the AIUB RD solution. The residual distribution is reduced to the level of +/- 20 mm for both ERD and KIN orbits, but with a more pronounced increase of observation residuals within the range +/- 4 mm for ERD orbits, and for TB+G and RB+TB+G solutions. Estimating troposphere corrections allows us to properly compare and verify the quality of satellite orbits because after removing systematic errors, the differences between KIN and RD orbits become most pronounced. Furthermore, introducing additional gradient corrections and range biases allows us to distinguish the quality of the orbits, however, the estimated parameters are inconsistent thus, may absorb orbital errors. Thus, RB+TB+G solutions fail to unambiguously differentiate the SLR errors from POD errors in the verification procedure. The solution RB+TB+G is overparameterized because introducing range biases insignificantly reduces the SLR residuals despite an increase in the number of estimated parameters. However, the high consistency of estimated troposphere parameters from TB solutions and POD-related verification results show that the orbit-related errors are not absorbed by tropospheric parameters. The TB solution allows us to properly verify different POD approaches, showing the high consistency of SLR observations with AIUB RB orbits, followed by ESA RD, and then AIUB KIN orbits.